

Single-source CVD routes to titanium phosphide

Christopher S. Blackman,^a Claire J. Carmalt,^{*a} Ivan P. Parkin,^a Leonardo Apostolico,^b Kieran C. Molloy,^b Andrew J. P. White^c and David J. Williams^c^a Department of Chemistry, Christopher Ingold Laboratories, University College London, 20 Gordon Street, UK WC1H 0AJ. E-mail: c.j.carmalt@ucl.ac.uk^b Department of Chemistry, University of Bath, Claverton Down, UK BA2 7AY^c Department of Chemistry, Imperial College of Science, Technology and Medicine, South Kensington, UK SW7 2AY

Received 12th April 2002, Accepted 7th May 2002

First published as an Advance Article on the web 28th May 2002

Treatment of TiCl_4 with two equivalents of L (L = PhPH_2 , Ph_2PH , PPh_3 , CyPH_2 , Cy_2PH , PCy_3) resulted in the formation of $[\text{TiCl}_4(\text{L})_2]$. Reaction of TiCl_4 with a stoichiometric amount of 1,2-bis(diphenylphosphino)methane (dppm), 1,2-bis(diphenylphosphino)ethane (dppe) and 1,2-bis(diphenylphosphino)propane (dppp) affords $[\text{TiCl}_4(\text{dppm})]$, $[\text{TiCl}_4(\text{dppe})]$ and $[\text{TiCl}_4(\text{dppp})]$, respectively. X-Ray crystal structures of $[\text{TiCl}_4(\text{Cy}_2\text{PH})_2]$ (**5**) and $[\text{TiCl}_4(\text{dppe})]$ (**9**) have been determined. Low pressure chemical vapour deposition (LPCVD) studies of all the compounds revealed that $[\text{TiCl}_4(\text{L})_2]$ (L = CyPH_2 , Cy_2PH and PCy_3) and $[\text{TiCl}_4(\text{dppm})]$ can form titanium phosphide thin-films on glass.

Introduction

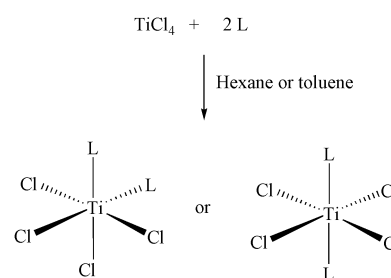
The formation of titanium(III) phosphide (TiP) thin films has received little attention, although this material possesses a number of useful properties. It is a metallic conductor, refractory (dec. < 1580 °C), hard and shows good resistance to oxidation at elevated temperatures.¹ Furthermore, thin films of early transition metal phosphides have been used as diffusion barriers in semiconductor devices.² Bulk TiP may be prepared by direct elemental combination³ or *via* the solid state metathesis reaction of TiI_4 with Na_3P .⁴ Alternatively, thin films of TiP have been prepared by chemical vapour deposition (CVD) involving the gas phase reaction of TiCl_4 and PCl_3 under an atmosphere of hydrogen and argon at 850–1050 °C.⁵ This route requires high reaction temperatures which in turn limits the choice of substrate used in the film deposition process. More recently, we have reported the first dual-source APCVD (atmospheric pressure CVD) route to TiP coatings on glass from the reaction of TiCl_4 and Bu^iPH_2 at 500–600 °C.⁶ Single-source precursors, which contain pre-formed Ti–P bonds, could offer several potential advantages over the dual-source routes, including lower deposition temperatures and easier handling of the precursors. However, to the best of our knowledge, only one single-source precursor to titanium phosphide thin films has been reported to date. Silver-coloured titanium phosphide films, of composition $\text{TiP}_{1.1}$ were grown on glass and silicon substrates using the precursor, $[\text{TiCl}_4(\text{CyPH}_2)_2]$, within the temperature range 350–600 °C.⁷

Herein we describe the synthesis and characterisation of a range of complexes of the type $[\text{TiCl}_4(\text{L})_2]$ (L = PhPH_2 , Ph_2PH , PPh_3 , CyPH_2 , Cy_2PH , PCy_3) and $[\text{TiCl}_4(\text{L}')]$ (L' = dppm, dppe, dppp). Two of the complexes, namely $[\text{TiCl}_4(\text{Cy}_2\text{PH})_2]$ and $[\text{TiCl}_4(\text{dppe})]$, have been structurally characterised. Low pressure chemical vapour deposition experiments on the complexes are described, enabling assessments to be made of the potential of the compounds to act as precursors to titanium phosphide thin films. We are particularly interested in investigating what effect changing the phosphine ligand has on the resulting film composition.

Results and discussion

Synthesis and characterisation

Treatment of TiCl_4 with two equivalents of a phosphine, L, resulted in the formation of $[\text{TiCl}_4(\text{L})_2]$ [L = PhPH_2 (**1**), Ph_2PH (**2**), PPh_3 (**3**), CyPH_2 (**4**), Cy_2PH (**5**); Cy = cyclohexyl, Ph = phenyl] in high yield (> 66%). All the complexes (**1–5**) have been characterised by ^1H and ^{31}P NMR, the results of which indicate that a monomeric complex $[\text{TiCl}_4(\text{L})_2]$ with either *cis*- or *trans*-phosphines has been isolated in all reactions (Scheme 1). To



Scheme 1 L = PhPH_2 (**1**), Ph_2PH (**2**), PPh_3 (**3**), CyPH_2 (**4**), Cy_2PH (**5**), Cy_3P (**6/7**).

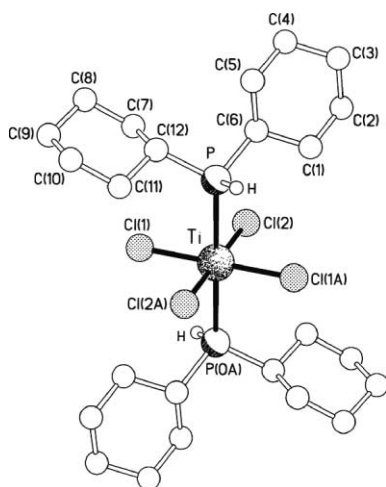
investigate whether the *cis* or *trans* isomer has been formed the X-ray crystal structure of compound **5** has been determined.

A crystal structure determination showed **5** to be the *trans* complex illustrated in Fig. 1. The molecule has crystallographic C_i symmetry and the geometry at titanium is slightly distorted octahedral having *cis* angles in the range 87.79(3) to 92.21(3)°. The Ti–Cl and Ti–P distances are unexceptional (Table 1). The shortest approach to the P–H hydrogen atom is an intermolecular contact of 3.34 Å to Cl(1). There are no other intermolecular contacts of note.

Analytical data were also obtained for compounds **1–5**. The carbon and hydrogen analyses for (**2**) and (**4**) were satisfactory. However, for compounds **1**, **3** and **5**, although the hydrogen analyses were satisfactory, the carbon analyses were consistently low by 1–3%. We presume that this observation is due

Table 1 Selected bond lengths (Å) and angles (°) for **5**

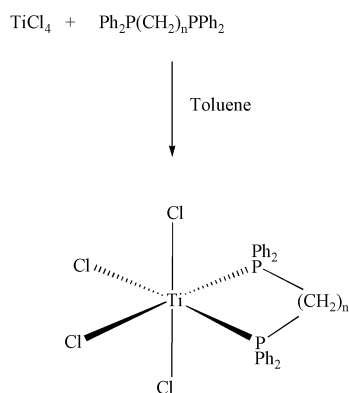
Ti–Cl(1)	2.2892(8)	Ti–Cl(2)	2.2837(8)
Ti–P	2.6372(8)		
Cl(2)–Ti–Cl(1)	89.00(3)	Cl(1)–Ti–Cl(2A)	91.00(3)
Cl(2)–Ti–P	90.75(3)	Cl(2A)–Ti–P	89.25(3)
Cl(1)–Ti–P	92.21(3)	Cl(1A)–Ti–P	87.79(3)
C(6)–P–C(12)	106.2(2)		

**Fig. 1** The molecular structure of **5**.

to the formation of either titanium phosphide with carbon impurities or metal carbide during the thermal decomposition stage of the microanalysis procedure. Attempts at improving the microanalysis by using a combustion aid were unsuccessful.

In contrast to the reactions described above, treatment of TiCl_4 with two equivalents of PCy_3 resulted in the isolation of a cream crystalline material. Analytical and spectroscopic data for these crystals are consistent with the formation of a mixture of two complexes, namely $[\text{TiCl}_4(\text{PCy}_3)_2]$ (**6**) and $[\text{TiCl}_4(\text{PCy}_3)]$ (**7**). Evidence for the formation of **6** and **7** was apparent from ^{31}P NMR where two signals were observed at +20.01 and +80.06 ppm. This result is not surprising given the bulky nature of the PCy_3 ligand.

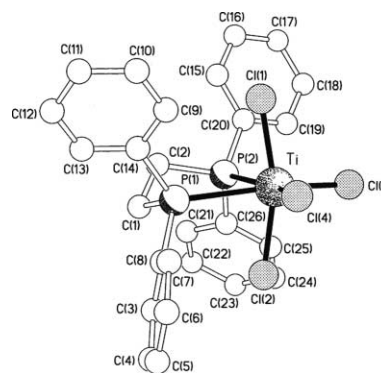
The related reactions between TiCl_4 and a stoichiometric amount of a chelating phosphine, L' , in toluene, resulted in the isolation of $[\text{TiCl}_4(\text{L}')]_2$ [where $\text{L}' = \text{dppm}$ (**8**), dppe (**9**) and dppp (**10**)]. Analytical and spectroscopic data for (**8**–**10**) were consistent with the proposed formula (Scheme 2) and an X-ray crystal structure was determined for **9**.

**Scheme 2** $\text{Ph}_2\text{P}(\text{CH}_2)_n\text{PPh}_2$: $n = 1$, 1,2-bis(diphenylphosphino)methane (dppm) (**8**); $n = 2$, 1,2-bis(diphenylphosphino)ethane (dppe) (**9**); $n = 3$, 1,2-bis(diphenylphosphino)propane (dppp) (**10**).

In the solid state complex **9** is seen to have approximate C_2 symmetry about an axis passing through the bisector of the equatorial $\text{Cl}(3)\text{--Ti--Cl}(4)$ and $\text{P}(1)\text{--Ti--P}(2)$ angles (Fig. 2). The geometry at titanium exhibits a distortion comparable to

Table 2 Selected bond lengths (Å) and angles (°) for **9**

Ti–Cl(1)	2.265(2)	Ti–Cl(2)	2.296(2)
Ti–Cl(3)	2.265(2)	Ti–Cl(4)	2.251(2)
Ti–P(1)	2.660(2)	Ti–P(2)	2.640(2)
Cl(4)–Ti–Cl(3)	107.74(7)	Cl(4)–Ti–Cl(1)	96.53(7)
Cl(3)–Ti–Cl(1)	96.57(7)	Cl(4)–Ti–Cl(2)	95.44(7)
Cl(3)–Ti–Cl(2)	92.78(7)	Cl(1)–Ti–Cl(2)	161.79(8)
Cl(4)–Ti–P(2)	163.12(6)	Cl(3)–Ti–P(2)	89.05(6)
Cl(1)–Ti–P(2)	79.31(6)	Cl(2)–Ti–P(2)	85.28(6)
Cl(4)–Ti–P(1)	86.92(6)	Cl(3)–Ti–P(1)	163.79(7)
Cl(1)–Ti–P(1)	88.36(6)	Cl(2)–Ti–P(1)	78.63(6)
P(2)–Ti–P(1)	76.66(5)		

**Fig. 2** The molecular structure of **9** showing the folding of the axial chloride ligands over the plane of the chelate ring.

those seen in titanium and hafnium octahedral complexes with 1,2-bisphosphinoethane⁸ having the two axial chloride ligands directed over the phosphine chelate ring—here the $\text{Cl}(1)\text{--Ti--Cl}(2)$ angle is $161.79(8)^\circ$. Other distortions include a folding by 0.39 \AA of one of the phosphorus atoms $[\text{P}(1)]$ out of the basal $\text{Ti}/\text{Cl}(3)/\text{Cl}(4)/\text{P}(2)$ plane (which is coplanar to within 0.02 \AA), an enlargement of the $\text{Cl}(3)\text{--Ti--Cl}(4)$ angle to $107.74(7)^\circ$ and a ligand bite angle of $76.66(5)^\circ$. All of these parameters are comparable to those seen in related structures.⁸ The Ti–P and Ti–Cl distances are again unexceptional (Table 2). The packing of the molecules is dominated by aromatic \cdots aromatic edge-to-face interactions with the edges of the C(20) and C(8) containing phenyl rings being directed orthogonally into the faces of the C(8) and C(14) containing rings respectively of neighbouring molecules; the associated ring centroid \cdots ring centroid separations are 5.05 and 5.13 \AA .

The octahedral coordination geometry around the titanium metal atom found in complexes **5** and **9** is unexceptional. Titanium tetrachloride readily forms adducts of the type TiCl_4L_n with donor ligands.⁹ The coordination numbers are generally five or six but in a few rare cases eight coordination has been found.¹⁰ Reaction of $\text{C}_2\text{H}_4(\text{PMe}_3)_2$ with TiCl_4 in the presence of diethylzinc produced $\text{TiCl}_4[\text{C}_2\text{H}_4(\text{PMe}_3)_2]_2$ with a distorted square antiprismatic geometry.¹⁰ Reid and co-workers have thoroughly investigated the coordination geometry of titanium(IV) halides with chelating phosphine and arsine ligands.¹¹ They noted that both six- and eight-coordinate complexes could be obtained. Notably the eight-coordinate complexes were formed with phosphines and arsines with relatively small cone angles at the metal; $o\text{-C}_6\text{H}_4(\text{PMe}_3)_2$ and $o\text{-C}_6\text{H}_4(\text{AsMe}_3)_2$ whereas the comparable six-coordinate species were formed with the more sterically demanding $\text{Ph}_2\text{PCH}_2\text{PPh}_2$ and $o\text{-C}_6\text{H}_4(\text{PPh}_3)_2$ species.¹¹ Considering the comparatively large size of PCy_2H and dppe it is not surprising that octahedral geometry is found for **5** and **9**. A search of the Cambridge structural data base revealed that **5** is the first crystallographically characterised $\text{TiCl}_4(\text{PR}_x)_2$ structure without a chelating phosphine ligand. The *trans* arrangement found for **5** does not indicate that all unidentate phosphines adopt this

geometry. Attempts at elucidating the geometries of the other complexes by IR spectroscopy, considering Ti–Cl stretches and P–H bands was difficult, primarily as the samples were exceedingly air sensitive and partially decomposed during the analysis. However preliminary IR analysis indicates that **4** has a *trans* geometry (two or less Ti–Cl stretches).

In order to study the decomposition pathway of compounds **1–10** and to assess their suitability as CVD precursors, thermal analyses were carried out. The TGA/DSC (thermal gravimetric analysis/differential scanning calorimetry) of **4** ($10\text{ }^{\circ}\text{C min}^{-1}$ from 20 to 500 $^{\circ}\text{C}$) shows a melt at 120 $^{\circ}\text{C}$ by DSC followed by a decomposition with an onset temperature of 200 $^{\circ}\text{C}$. The decomposition of **4** is clean and shows a weight loss of 50%. This behaviour indicates an incomplete decomposition to TiP up to 500 $^{\circ}\text{C}$. All the other complexes show similar behaviour with a weight loss of between 50 and 60%.

Chemical vapour deposition studies

Low pressure chemical vapour deposition of **1–10** were investigated.¹² No films were deposited from compounds **1**, **2**, **3** or **10** because the precursor either decomposed before volatilisation, or it carried through the hot zone without depositing a film. From compounds **4**, **5**, **6/7**, **8** and **9**, two types of film were deposited – as shown by an initial survey study of the film formed on the curved surface of a hot-wall glass-tube and a thorough depth-composition analysis of the films formed on small glass plates ($5 \times 0.5\text{ cm}$) placed inside of the glass tube.

The films produced by CVD varied in colour, as shown in Table 3. The titanium phosphide films produced from **4** and **5** are resistant to attack by common solvents, for example toluene, acetone and tetrahydrofuran. However, concentrated nitric acid digested the film from **4** and partly digested the film from **5**, after four weeks immersion. Concentrated hydrochloric acid completely digested the films after one week's immersion. All the films passed the Scotch tape test. The films were also hard and could not be scratched with a brass stylus and in some cases with a stainless steel scalpel. The silver and gold TiP films formed from **4** and **5** were electrically conducting with sheet resistance measurements of $2\text{--}7\text{ }\Omega\text{ }\square^{-1}$. The black films were more electrically insulating. All of the films had contact angles for the spread of a water droplet in the region of $48\text{--}90^{\circ}$. These values are very close to that of uncoated glass of 70° and indicate a hydrophobic surface.

The films produced on curved glass were analysed by Energy Dispersive Analysis by X-rays (EDAX) and Scanning Electron Microscopy (SEM), electron probe and Raman spectroscopy. The EDAX data showed the presence of titanium and phosphorus in the films produced from compounds **4**, **5**, **6/7** and **8**, but only titanium (no P) in the film from **9**. Significant breakthrough of the excitation volume through the coating to the underlying glass was observed in most cases and so accurate quantitative analysis by EDAX was difficult. However, electron probe measurements showed that the composition of the titanium phosphide films deposited *appeared* to change from $\text{Ti}_{1.1}\text{P}$ to Ti_3P (Table 3, *vide infra*).¹⁰ The formation of $\text{Ti}_{1.1}\text{P}$ from compound **4** is in contrast with a previous report, where $\text{TiP}_{1.1}$ films were grown from **4** in the temperature range $350\text{--}600\text{ }^{\circ}\text{C}$.⁷

The Raman spectrum of the film grown on curved glass from **4** (Fig. 3) is very similar to that obtained for bulk TiP with major bands occurring at 234 and 305 cm^{-1} . The film grown from compound **6/7** produced a different Raman spectrum with broad peaks occurring at 432 and 631 cm^{-1} and a weak peak at 151 cm^{-1} . The film grown from **9** showed the formation of $\text{Ti}_{1.6}\text{P}$ from EDAX measurements. Despite this, the Raman spectrum of this film indicates that the anatase phase of TiO_2 has been produced. It is possible that a TiP film was formed during the CVD reaction and surface oxidation has occurred on exposure to air, or that an oxide was formed during the CVD

Table 3 Analysis of the films formed in the CVD process

Sample	Film colour on curved glass	Electron probe results on curved glass	Raman from flat glass	Film colour from flat glass	EDAX results from flat glass	Raman on flat glass	XRD on flat glass	Conductance/ $\Omega\text{ }\square^{-1}$	Scratch tests ^c	Contact angle/ $^{\circ}$	XPS/RBS analysis
$[\text{TiCl}_4(\text{PCyH}_2)_2]\text{ (4)}$	Silver	$\text{Ti}_{1.1}\text{P}$	TiP	Gold	$\text{Ti}_{1.3}\text{P}$ C ~ 0% Cl ~ 5%	TiP	Amorphous	2	Failed diamond	80	Top 140 nm $\text{Ti}_{1.0}\text{P}_{0.5}\text{O}_{0.5}\text{C}_{0.5}\text{Cl}_2$ Bulk of film TiP _{1.05}
$[\text{TiCl}_4(\text{PCy}_2\text{H})_2]\text{ (5)}$	Gold	$\text{Ti}_{1.7}\text{P}$	—	Black/gold	$\text{Ti}_{1.4}\text{P}$ C ~ 3% Cl ~ 5%	TiP	Amorphous	7	Failed steel	87	Top 500 nm TiPOC Bottom 800 nm TiP
$[\text{TiCl}_4(\text{PCy}_3)_2]\text{ (6)}$ $[\text{TiCl}_4(\text{PCy}_3)]\text{ (7)}$	Black	Ti_2P^a	? ^b	Black	Ti	TiO_2	Amorphous	Insulating	Failed brass	48	
$[\text{TiCl}_4(\text{dppm})]\text{ (8)}$	Gold	Ti_3P	? ^b	Dull gold	$\text{Ti}_{2.1}\text{P}$ C ~ 80% Cl ~ 1%	No pattern	Amorphous	260	Failed brass	66	TiO_2 and TiP layers
$[\text{TiCl}_4(\text{dppe})]\text{ (9)}$	Gold	Ti	TiO_2	Shiny black	$\text{Ti}_{1.6}\text{P}$ C ~ 40% Cl ~ 2%	TiO_2	Amorphous	300	Failed brass	66	TiP and TiO_2 layers

^a EDAX measurement not electron-probe. ^b Further experiments have shown that the unclassified Raman spectra is typical of poor quality TiO_2 . ^c Hardness scratch tests in order; paper towel, felt cloth, brass, stainless steel, diamond. Failed diamond means that the film passed all of the lower tests.

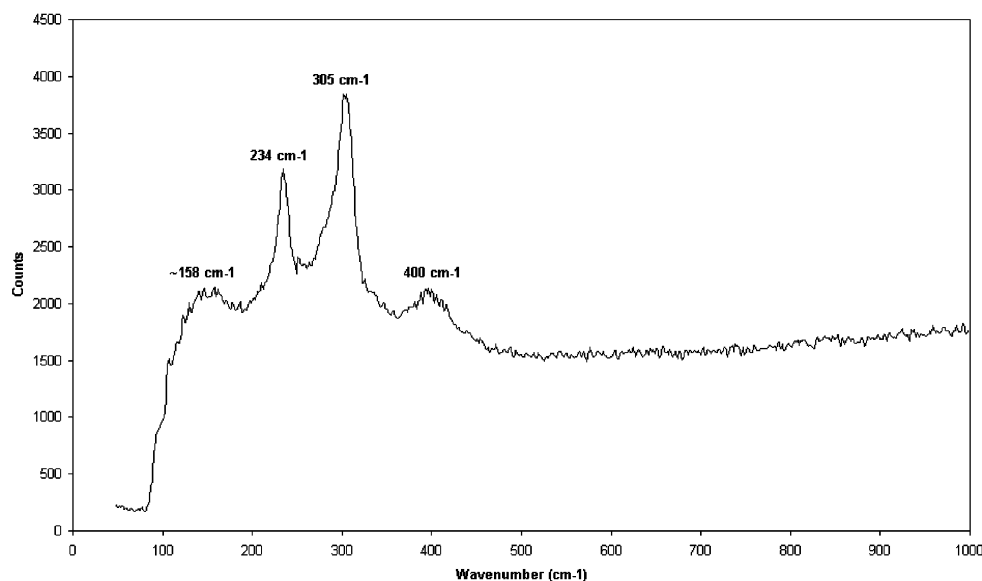


Fig. 3 Raman spectrum of the film grown from compound 4.

process. By Scanning Electron Microscopy (SEM) the film grown from **5** shows spherical particles of size 200 nm which are aggregated together to form a film (Fig. 4). The $\text{Ti}_{1.1}\text{P}$ film grown from compound **4** had similar spherical particles, indicative of some degree of gas-phase nucleation (Fig. 5). Because

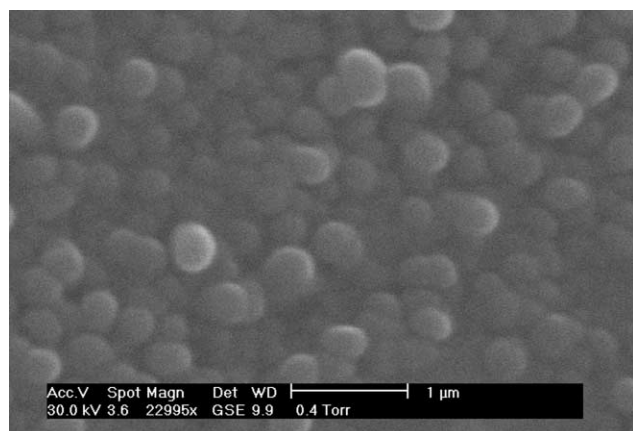


Fig. 4 SEM of the film produced by the decomposition of **5**.

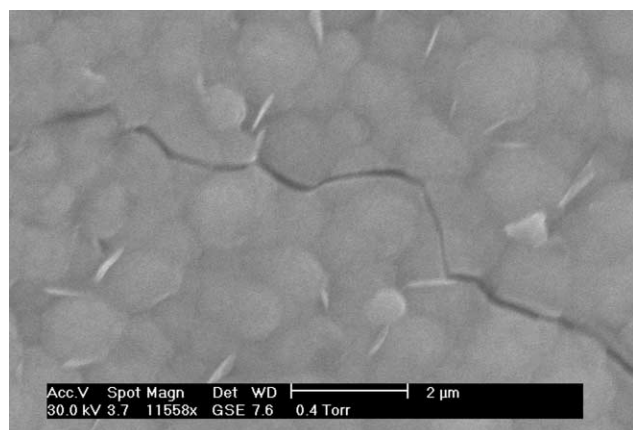


Fig. 5 SEM of the film produced by the decomposition of **4**.

of the somewhat contradictory nature of the film analysis on curved glass (e.g. TiO_2 by Raman and $\text{Ti}_{1.6}\text{P}$ by EDAX) a second set of depositions was conducted on flat glass using the same CVD procedure. In this case formation of a film on

flat glass enabled a more detailed analysis by depth profiling techniques.

Film analysis on flat glass; depth profiling studies

Reactions were conducted in the same way for the curved glass samples with the exception that small pieces of glass were inserted into the glass tube. Deposition was noted on both the top and bottom surfaces of the glass substrates. Use of flat substrates enabled more detailed analysis by XPS, Rutherford backscattering and X-ray powder diffraction. Notably, the flat surface depositions were some 50–100 °C lower in temperature than the curved wall experiments for the same set oven temperature of 550 °C.

Electron probe results on curved glass samples showed almost stoichiometric TiP was formed from **4**. Raman showed a TiP spectrum. EDAX analysis of film deposited onto flat glass showed a slightly titanium rich phase. The film was amorphous by powder XRD. Rutherford backscattering spectra (RBS) showed a surface layer of mixed products with a film of $\text{Ti}_1\text{P}_{1.05}$ underneath (Fig. 6). The surface layer was 140 nm thick and

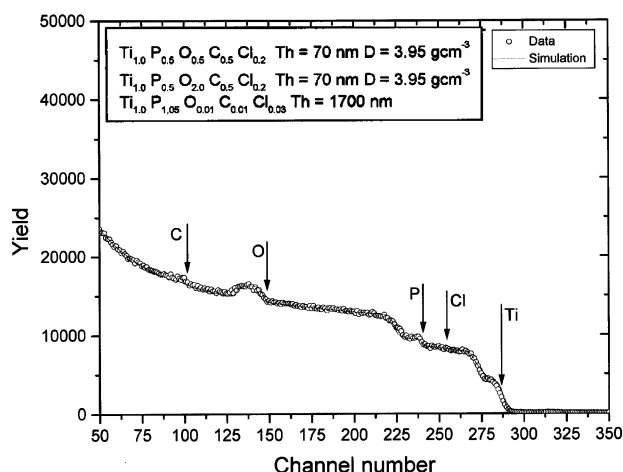


Fig. 6 Rutherford backscattering spectrum of the surface layer of the film formed from the CVD of **4**.

had composition $\text{Ti}_{1.0}\text{P}_{0.5}\text{O}_{0.5}\text{C}_{0.5}\text{Cl}_2$, the bulk of the film was 1700 nm thick of formula $\text{Ti}_{1.00}\text{P}_{1.05}$ with almost undetectable levels of carbon and chlorine contamination. Film thickness from RBS gave a growth rate during the CVD process of ca. 400 nm h⁻¹. The X-ray photoelectron spectra of the film

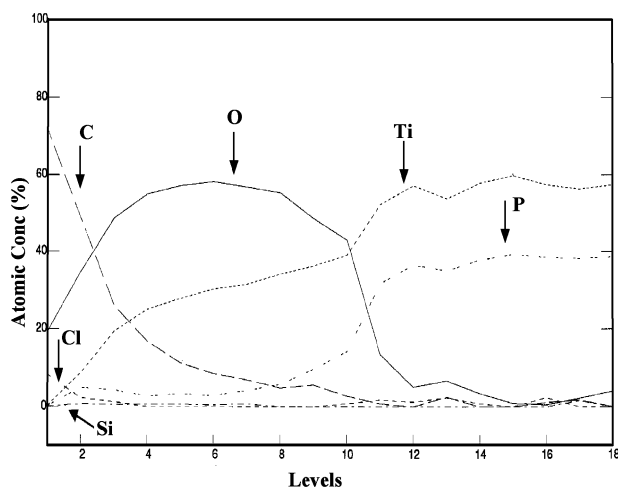


Fig. 7 X-Ray photoelectron spectroscopy depth-profile analysis of the film formed from the CVD of **4**.

from **4** was fully consistent with the RBS results. It can be seen from the elemental composition by XPS that there is a surface layer containing mostly titanium and oxygen (Fig. 7). Sputtering reduces the carbon in this portion of the film and phosphorus begins to be revealed. There is an abrupt junction where the film composition changes to containing only titanium and phosphorus. The atomic concentration for titanium is slightly misleading due to problems in accurately integrating the Ti $2p_{3/2}$ peaks. Analysis of the binding energies showed that at the surface the Ti $2p_{3/2}$ binding energy was 459.0 eV (TiO_2 is 458.7 eV)¹² although the shift for TiPO_4 is in an almost identical location¹³, suggesting oxide or phosphate. The O 1s peak is centred on 531.2 eV (TiO_2 is 530.6 eV and PO_4^{3-} is 532.4 eV but for titanium PO_4^{3-} it is difficult to differentiate from oxide).¹³ The P 2p peak is invisible on the surface but sputtering reveals a small peak centred on 133.8 eV (PO_4^{3-} is 133.9 eV)¹³ for the first few sputtered layers. This suggests that the surface is TiO_2 and the first few sputtered layers are mainly TiO_2 with a small amount of phosphate present (from atomic concentrations). The phosphorous atomic concentration is growing at around level 8 as a large P 2p peak centred on 128.8 eV is revealed (TiP is 128.6 eV).¹⁴ The Ti $2p_{3/2}$ peak through these levels is broad and poorly shaped suggesting a mixture of TiO_2 , TiPO_4 and TiP. After the abrupt junction at level 10 only a Ti 2p peak at 454.6 eV is visible (TiP 454.6 eV) and a P 2p peak at 128.8 eV (TiP 128.6 eV). In the TiP layer there was undetectable chlorine contamination and almost undetectable carbon contamination.

Winter has reported a similar LPCVD reaction for the formation of TiP films from **4** on silicon and glass substrates.⁷ Notably the films obtained were X-ray amorphous. Analysis by XPS and RBS revealed a composition of $\text{TiP}_{1.1}$ with no chlorine or carbon contamination. This compares very favourably with the results that were obtained in this study.

Electron probe results from the vapour phase experiment on curved glass on **5** showed a stoichiometry of $\text{Ti}_{1.7}\text{P}$. EDAX analysis of the film on flat glass showed a slightly more phosphorus rich stoichiometry ($\text{Ti}_{1.44}\text{P}$) with more carbon present than detected in the film produced from CyPH_2 **4**. Raman spectroscopy of **5** showed a characteristic TiP spectrum. The film was amorphous by XRD. RBS analysis of the film showed two distinct regions. The top *ca.* 500 nm was of variable composition but was consistently metal rich with significant oxide and carbon contamination. A second region was *ca.* 800 nm thick and was stoichiometric TiP. Oxide and carbon contamination were reduced in the second layer but not eliminated. There was almost undetectable chlorine contamination in either layer. XPS analysis was used to examine the film further,

although, complete etching through to the substrate was not achieved. Surface carbon contamination reduced over subsequent etches to almost nothing. The surface layers show a Ti $2p_{3/2}$ binding energy of 458.8 eV, indicative of oxide or phosphate, although there is almost no phosphorus detected at the surface suggesting an overlayer of TiO_2 . There was significant oxygen contamination in the layers examined however the second layer shown by RBS was not etched into. This is because the etching-gun could only remove *ca.* 300 nm in a meaningful timescale (8 h). The O 1s peak was extremely broad and encompassed two peaks, one at 531 eV (oxide)¹² and 532.8 eV (phosphate).¹³ This peak remained through all the etched layers. However, after etching the only visible P 2p peak was centred at 128.6 eV (TiP)¹⁴ and the only visible Ti $2p_{3/2}$ was at 454.4 eV although the peak shape was poor. The Ti $2p_{3/2}$ and P 2p peaks show evidence of oxide/phosphate and phosphate presence respectively but these are extremely minor compared to the phosphide peaks.

Electron probe analysis of the film produced from **8** on curved glass gave a composition of Ti_3P . Raman analysis showed a low quality TiO_2 spectrum. EDAX analysis of the film deposited on flat glass gave a stoichiometry of $\text{Ti}_{2.1}\text{P}$ although the amount of titanium and phosphorus was very low with significant breakthrough to the underlying glass substrate. EDAX also revealed that the film had considerable amounts of carbon although the amount of chlorine present was low (*ca.* 1%). This amount of carbon probably accounts for the colour of the film. RBS analysis indicated a relatively thin film (*ca.* 160 nm) with a fixed composition of TiP. X-ray photoelectron spectroscopy showed no surface titanium or phosphorus peaks and showed only the presence of a carbon film. Sputtering reduced the amount of carbon in the film but it remained significant until the substrate was reached. Sputtering also revealed a Ti $2p_{3/2}$ peak with a binding energy of 454.7 eV (TiP)¹² and a phosphorus peak at 128.8 eV (TiP).¹⁴ There was little sign of contamination with oxygen in either oxide or phosphate form. Combination of this data is probably best interpreted by the formation of the TiP phase that was contaminated with TiO_2 at the surface and by carbon throughout the film.

Electron probe analysis of the film produced from vapour phase experiments of **9** gave a composition indicative of a TiO_2 film. The Raman spectrum obtained for this sample was that of TiO_2 . EDAX analysis of the film on flat glass showed a $\text{Ti}_{1.6}\text{P}$ stoichiometry with heavy carbon contamination (40%) although only slight chlorine contamination (2%). XPS showed surface Ti $2p_{3/2}$ binding energy of 458.8 eV (TiO_2 is 458.7 eV although TiPO_4 is similar), a P 2p binding energy of 133.4 eV (PO_4^{3-} is 133.9 eV) and an O 1s binding energy of 532.2 eV (PO_4^{3-} is 532.4 eV). This would suggest a titanium phosphate terminated surface. The first etched layers reveal a Ti $2p_{3/2}$ binding energy principally centred on 454.8 eV (TiP 454.6 eV) and a P 2p energy of 128.4 eV (TiP 128.8 eV). Further etching rapidly reduced the P 2p peak and reveals a broad poorly formed Ti 2p peak indicative of oxide. The O 1s peak observed at this region is centred at 530.6 eV (TiO_2 530.6 eV).

Summary of the depth profile analysis

The depth profiling studies of **4**, **5**, **8** and **9** all reveal that the samples show a change in composition with depth. The bulk film in most cases is TiP. The top layers of the films contain the most oxide. This is fully consistent with the films undergoing some post reaction oxidation upon storage in air. If an ingress of oxygen occurred during the CVD process then the oxygen content would be expected to be uniform with depth throughout the sample. The formation of the oxide coating on the surface probably accounts for why these films are so resistant to solvents and acids. Notably none or negligible amounts of chlorine were detected in the films indicating that it is fully

removed during the deposition stage. This is relatively unusual especially for the studies of **8** and **9** where no active hydrogen is present on the phosphine ligands. Notably the amount of carbon seen in some of the films was considerable. This could be directly correlated with the nature of the phosphine ligand. The higher the carbon content of the starting phosphine on the adduct and the lower its number of active hydrogens the more carbon was found in the film. Interestingly even in the highly carbon contaminated films the titanium and phosphorous seem to present as stoichiometric TiP from XPS measurements.

The seemingly contradictory film analysis from the different techniques is easily reconciled. XPS interrogates only the first ten or so atomic layers of the surface. Hence, by combining XPS analysis with sputtering to remove *ca.* 20 nm thickness segments from the surface individual layers can be examined, much like looking at different layers in an onion. Thus XPS revealed changes in composition with depth. The RBS functions in a somewhat similar fashion. The EDX and electron probe measurements rely on ejected X-rays for analysis. At the accelerating voltages used in the experiments typical penetration depths were 1–2 μm . Hence the EDAX and electron probe measurements consistently gave titanium rich films in a number of cases. This was because the total titanium count was made up from the surface titanium oxide as well as the bulk titanium phosphide phases. The phosphorus count was made up primarily from the titanium phosphide although some surface phosphate was also possible. Thus it is likely that only TiP was formed as the Ti phase in these reactions and the analysis that indicated Ti_2P *etc.* on the curved glass samples was misleading as to the true nature of the films.

All of the films formed on flat glass were amorphous by X-rays. This is probably not too surprising as the surface looks to have been oxidised in all cases. Further the temperature of deposition on the flat glass plates was some 50 $^\circ\text{C}$ lower than the walls of the glass that was analysed in the curved glass experiments.

Aspects of film analysis

We have shown previously that titanium dioxide surfaces show photo-assisted hydrophilicity.¹⁵ This can be assessed by determination of the contact angle of a water droplet on the coated surface. In the titanium phosphide films formed in these experiments the initial films gave contact angles in the range 48–80 $^\circ$, notably the contact angles did drop on photo-irradiation by 5–10 $^\circ$. This is not as great as that expected for a pure TiO_2 that can drop by 60–70 $^\circ$ but is still in line with a TiO_2 surface. Notably the film from **6/7** had the most readily identified TiO_2 surface from Raman analysis and the lowest contact angle measurement.

The attempted CVD of **1**, **2**, **3** or **10**, all of which contained a phenyl substituent on the phosphorus atom, resulted in failure. In most cases transport of the precursor through the hot zone of the CVD experiment did occur. However, an oily material was seen in the colder sections of the reaction tube past the hot zone. It is thus possible that the temperatures employed in these experiments and the residence time of the precursor in the reaction tube is such that film growth does not occur. It is tempting to speculate that in the Cy derivatives **4** and **5** cyclohexene is eliminated in the reaction pathway, indeed this has been observed by Winter in a related reaction.⁷ In the corresponding phenyl cases a similar pathway *via* a benzyne intermediate would be expected to be less favoured.

A dual source CVD route to TiP films on glass has been reported from the reaction of TiCl_4 and Bu^iPH_2 .⁶ The product was of high purity and equivalent in colour, composition and physical properties to that observed here from the single source CVD of **4**. Notably in both cases a monoalkylphosphine was employed in the CVD experiment. The single source route has some appeal in that the reaction uses inexpensive and con-

siderably less complicated apparatus. However, the prior synthesis and isolation of an air sensitive precursor are notable problems with the single source route. Further the use of other secondary or tertiary phosphines, although somewhat successful, produces films with extensive carbon contamination. Thus the strategy of employing primary phosphines in an extension of this work to other metals would be the most promising avenue to pursue.

The degree of oxidation noted at the surface of all of the films appears to happen quite rapidly after exposure of the film to air. However the processes seems to be self-limiting because the oxide layer formed on the films from **4** and **5** did not seem to progress further into the solid on storage in air for six months as the optical properties were invariant with time and reanalysis indicated an unchanged material.

Conclusions

A range of complexes of the type $[\text{TiCl}_4(\text{L})_2]$ ($\text{L} = \text{PhPH}_2$, Ph_2PH , PPh_3 , CyPH_2 , Cy_2PH , PCy_3) and $[\text{TiCl}_4(\text{L}')]$ ($\text{L}' = \text{dppm}$, dppe or dppp) have been synthesised and characterised. Two of the complexes, namely $[\text{TiCl}_4(\text{Cy}_2\text{PH})_2]$ and $[\text{TiCl}_4(\text{dppe})]$ have been structurally characterised. Vapour phase thin-film studies indicate that $[\text{TiCl}_4(\text{L})_2]$ ($\text{L} = \text{CyPH}_2$, Cy_2PH and PCy_3) and $[\text{TiCl}_4(\text{dppm})]$ are effective titanium phosphide precursors whereas $[\text{TiCl}_4(\text{L})_2]$ ($\text{L} = \text{PhPH}_2$, Ph_2PH and PPh_3) and $[\text{TiCl}_4(\text{dppp})]$ did not produce a film under the same conditions. Interestingly, $[\text{TiCl}_4(\text{dppe})]$ produced a film containing only titanium (no P) under similar conditions. These results suggest that the complexes with primary or secondary phosphines (CyPH_2 and Cy_2PH) are superior titanium phosphide precursors.

Experimental

General procedures

All manipulations were performed under a dry, oxygen-free dinitrogen atmosphere using standard Schlenk techniques or in a Mbraun Unilab glove box. All solvents were distilled from appropriate drying agents prior to use (sodium/benzophenone for toluene, THF and hexanes; CaH_2 for CH_2Cl_2). All other reagents were procured commercially from Aldrich and used without further purification. Microanalytical data were obtained at University College London (UCL).

Physical measurements

^1H and ^{31}P NMR spectra were recorded on a Bruker AMX400 spectrometer at UCL. The NMR spectra are referenced to CDCl_3 , which was degassed and dried over molecular sieves prior to use; ^1H chemical shifts are reported relative to SiMe_4 (0.00 ppm); ^{31}P chemical shifts are reported relative to external 85% H_3PO_4 . IR spectra were recorded on a Nicolet 205 instrument. EDAX/SEM results were obtained on a JOEL 35-CF instrument using ISIS software (Oxford Instruments). Raman spectra were acquired on a Renishaw Raman System 1000 using a helium–neon laser of wavelength 632.8 nm. The Raman system was calibrated against the emission lines of neon. Electron microprobe analyses were obtained on a Jeol 8600 instrument and referenced against phosphorus and titanium standards. TGA of the compounds were obtained from the Thermal Methods Laboratory at Birkbeck College (ULIRS). Rutherford back scattering was obtained in association with Professor Colligon at the University of Salford. X-Ray powder diffraction patterns were measured on a Philips X-pert diffractometer using unfiltered ($\text{CuK}_{\alpha 1} \lambda = 1.5045 \text{ \AA}$, $\text{K}_{\alpha 2} \lambda = 1.5443 \text{ \AA}$) radiation in the reflection mode using glancing angle incidence. Samples were indexed using the Unit Cell program and compared to database standards. SEM/EDAX was obtained on a Hitachi S570 instrument using the KEVEX system. X-Ray

photoelectron spectra were recorded with a VG ESCALAB 220i XL instrument using focussed (300 μm spot) monochromatic Al-K α radiation at a pass energy of 20 eV. Scans were acquired with steps of 50 meV. A flood gun was used to control charging and the binding energies were referenced to an adventitious C 1s peak at 284.8 eV. Depth profile measurements were obtained by using argon beam sputtering. Contact angle measurements of selected glass samples were determined by measuring the spread of a 7.5 μl droplet of water and applying a suitable program. Electrical conductivity was determined by a four-probe device.

Preparations

[TiCl₄(PhPH₂)₂] (1). PhPH₂ (0.25 cm³, 2.50 mmol) was added to a solution of TiCl₄ (1 cm³, 1.0 M solution in toluene) in hexane (25 cm³). A yellow/orange solid began to precipitate immediately. The precipitate was isolated by filtration, washed with hexanes (3 \times 10 cm³) and dried *in vacuo* (0.27 g, 66%). Anal. Calc. For C₁₂H₁₄Cl₄P₂Ti: C, 35.16; H, 3.44. Found C, 33.26; H, 3.46. ³¹P{¹H} NMR (CDCl₃): δ -72.35 (s), $J_{\text{H-P}}$ = 308 Hz. ¹H NMR (CDCl₃): δ 4.96 (d, 4H, PhPH₂), 7.37–7.51 (m, 10H, PhPH₂).

A similar method to that described above for **1** was adopted for the synthesis of all the other complexes. The quantities used in each preparation are given below.

[TiCl₄(Ph₂PH)₂] (2). TiCl₄ (3 cm³, 1.0 M solution in toluene), Ph₂PH (1 cm³, 6.00 mmol), hexanes (40 cm³). An orange solid resulted. Anal. Calc. For C₂₄H₂₂Cl₄P₂Ti: C, 51.24, H 3.91. Anal. Calc. For C₂₄H₂₂Cl₄P₂Ti·(C₇H₈)_{0.5}: C, 54.31; H, 4.31. Found C, 54.04; H, 3.72. ³¹P{¹H} NMR (CDCl₃): δ -5.39 (s), $J_{\text{H-P}}$ = 330 Hz. ¹H NMR (CDCl₃): δ 5.57 (d, 2H, PhPH₂), 7.28–7.56 (m, 20H, PhPH₂).

[TiCl₄(PPh₃)₂] (3). TiCl₄ (5 cm³, 1.0 M solution in toluene), Ph₃P (2.62 g, 1.00 mmol), hexanes (50 cm³). A red solid resulted (3.1 g, 87%). Anal. Calc. For C₃₆H₃₀Cl₄P₂Ti: C, 60.53; H, 4.23. Found C, 57.68; H, 4.01. ³¹P{¹H} NMR (CDCl₃): δ 7.53 (s). ¹H NMR (CDCl₃): δ 7.36–7.71 (m, 20H, PhPH₂).

[TiCl₄(CyPH₂)₂] (4). TiCl₄ (5 cm³, 1.0 M solution in toluene), CyPH₂ (1.3 cm³, 1.00 mmol), hexanes (40 cm³). A yellow solid resulted (2.0 g, 96%). Anal. Calc. For C₁₂H₂₆Cl₄P₂Ti: C, 34.15; H, 6.21; Cl, 33.65. Found C, 34.08; H, 5.87; Cl, 34.94. ³¹P{¹H} NMR (CDCl₃): δ -39.71 (s), $J_{\text{H-P}}$ = 314 Hz. ¹H NMR (CDCl₃): δ 4.07 (d, 4H, CyPH₂), 1.19–2.18 (m, 22H, CyPH₂). IR (Ti-Cl) 350 cm⁻¹.

[TiCl₄(Cy₂PH)₂] (5). TiCl₄ (2.5 cm³, 1.0 M solution in toluene), Cy₂PH (1 cm³, 5.00 mmol), hexanes (25 cm³). A pink solid resulted (1.47 g, 100%). Anal. Calc. For C₂₄H₄₆Cl₄P₂Ti: C, 49.17; H, 7.91. Found C, 48.80; H, 8.36. ³¹P{¹H} NMR (CDCl₃): δ 20.33 (s), $J_{\text{H-P}}$ = 318 Hz. ¹H NMR (CDCl₃): δ 3.99 (d, 2H, Cy₂PH), 1.16–2.66 (m, 44H, Cy₂PH). Crystals suitable for X-ray crystallography were obtained by solvent diffusion of hexanes into a concentrated CH₂Cl₂ solution of **5** at room temperature over a number of days.

[TiCl₄(PCy₃)₂] (6)/[TiCl₄(PCy₃)₂] (7). TiCl₄ (1 cm³, 1.0 M solution in toluene), PCy₃ (0.56 g, 2.00 mmol), hexanes (40 cm³). A cream solid resulted (0.51 g, 68%, based on the formation of **7**). Anal. Calc. For C₃₆H₆₆Cl₄P₂Ti: C, 57.61; H, 8.86. Anal. Calc. For C₁₈H₃₃Cl₄P₂Ti: C, 45.99; H, 7.07. Found C, 49.28; H, 7.63. ³¹P{¹H} NMR (CDCl₃): δ 80.06 (s), 20.01 (s). ¹H NMR (CDCl₃): δ 1.18–2.57 (m, PCy₃).

[TiCl₄(dppm)] (8). TiCl₄ (2.5 cm³, 1.0 M solution in toluene), dppm (0.94 g, 2.5 mmol), toluene (25 cm³). An orange solid resulted. Anal. Calc. For C₂₅H₂₂Cl₄P₂Ti: C, 52.30; H, 3.86.

Found C, 54.50; H, 4.26. ³¹P{¹H} NMR (CDCl₃): δ -14.60 (s), $J_{\text{H-P}}$ = 10 Hz. ¹H NMR (CDCl₃): δ 3.98 (t, 2H, CH₂), 7.34–7.66 (m, 20H, Ph).

[TiCl₄(dppe)] (9). TiCl₄ (2.5 cm³, 1.0 M solution in toluene), dppe (0.99 g, 2.5 mmol), toluene (25 cm³). An orange solid resulted. Anal. Calc. For C₂₆H₂₄Cl₄P₂Ti: C, 53.10; H, 4.11. Anal. Calc. For C₂₆H₂₄Cl₄P₂Ti·(CH₂Cl₂)_{0.5}: C, 50.47; H, 4.00. Found C, 49.57; H, 4.06. ³¹P{¹H} NMR (CDCl₃): δ 20.80 (s). ¹H NMR (CDCl₃): δ 2.92–3.02 (m, 2H, CH₂), 7.19–7.73 (m, 20H, Ph). Crystals suitable for X-ray crystallography were obtained by solvent diffusion of hexanes into a concentrated CH₂Cl₂ solution of **9** at room temperature over a number of days.

[TiCl₄(dppp)] (10). TiCl₄ (2.5 cm³, 1.0 M solution in toluene), dppp (1.02 g, 2.5 mmol), toluene (25 cm³). An orange solid resulted. Anal. Calc. For C₂₇H₂₆Cl₄P₂Ti: C, 53.86; H, 4.35. Found C, 52.75; H, 4.00. ³¹P{¹H} NMR (CDCl₃): δ -1.85 (s). ¹H NMR (CDCl₃): δ 2.16–2.23 (m, 2H, CH₂), 2.68–2.71 (m, 4H, CH₂), 7.29–7.65 (m, 20H, Ph).

Chemical vapour deposition experiments

CVD experiments were conducted inside of a glass tube of length 50 cm and internal diameter 1 cm. The tube was evacuated to *ca.* 10⁻² Torr. Small glass plates (5 cm \times 0.5 cm) made from (BDH standard) microscope slides were inserted inside of the glass tube. The glass tube was placed inside of a tube furnace. The central portion of the tube was heated to 550 $^{\circ}\text{C}$ and the end containing the precursor heated to 100–150 $^{\circ}\text{C}$. The experiments were typically conducted for 4 h. A film was formed in the central portion of the glass tube, both on the walls of the tube and on the inserted microscope slides. After the deposition, the glass was allowed to cool to room temperature, the vacuum was turned off and the system exposed to air. The walls of the glass tube were broken and the film formed on the inside surface of the glass was examined, as was the film that had formed on the microscope slides.

X-Ray crystallography

Crystals of **5** and **9** were grown CH₂Cl₂–hexanes mixtures at room temperature. X-Ray analysis used the SHELXTL PC system for structural refinement.¹⁶

Crystal data for 5. C₂₄H₂₆P₂Cl₄Ti, M = 586.3, monoclinic, $P2_1/c$ (no. 14), a = 10.982(1), b = 10.169(1), c = 13.332(1) Å, β = 103.42(1) $^{\circ}$, V = 1448.2(1) Å³, Z = 2 (C_i symmetry), D_c = 1.344 g cm⁻³, $\mu(\text{Cu-K}\alpha)$ = 7.02 mm⁻¹, T = 203 K, orange/red plates; 2153 independent measured reflections, F^2 refinement, R_1 = 0.048, wR_2 = 0.124, 1899 independent observed absorption corrected reflections [$|F_o| > 4\sigma(|F_o|)$, $2\theta \leq 120^{\circ}$], 147 parameters. CCDC reference number 185882.

Crystal data for 9. C₂₆H₂₄P₂Cl₄Ti, M = 588.1, monoclinic, $P2_1/c$ (no. 14), a = 12.229(2), b = 14.560(2), c = 16.047(4) Å, β = 111.25(1) $^{\circ}$, V = 2662.8(7) Å³, Z = 4, D_c = 1.467 g cm⁻³, $\mu(\text{Cu-K}\alpha)$ = 7.66 mm⁻¹, T = 183 K, orange platey needles; 3294 independent measured reflections, F^2 refinement, R_1 = 0.055, wR_2 = 0.131, 2429 independent observed absorption corrected reflections [$|F_o| > 4\sigma(|F_o|)$, $2\theta \leq 114^{\circ}$], 251 parameters. CCDC reference number 185883.

See <http://www.rsc.org/suppdata/dt/b2/b203613b/> for crystallographic data in CIF or other electronic format.

Acknowledgements

The EPSRC is thanked for grant GR/M98623 (I. P. P. and C. J. C.) and GR/M98630 (K. C. M.). C. J. C. is also grateful to the Royal Society for a Dorothy Hodgkin fellowship and

research grant. Pilkington Glass are thanked for the glass substrates and Epichem Ltd for phosphines. Professor R. J. H. Clark is thanked for help with the Raman spectra and the EPSRC for grant GR/M82592 for purchase of the Raman spectrometer.

References

- 1 R. L. Ripley, *J. Less Common Met.*, 1962, **4**, 496; B. Nolang, O. Eriksson and B. Johansson, *J. Solid State Chem.*, 1990, **86**, 300.
- 2 K. Komaki, Japanese Patent JP 02 248 079, 1990.
- 3 T. Lundstrom and P. O. Snell, *Acta Chem. Scand.*, 1967, **21**, 1343.
- 4 R. F. Jarvis, R. M. Jacubinas and R. B. Kaner, *Inorg. Chem.*, 2000, **39**, 3243.
- 5 S. Motojima, T. Wakamatsu and K. Sugiyama, *J. Less Common Met.*, 1981, **82**, 379.
- 6 C. Blackman, C. J. Carmalt, S. A. O'Neill, I. P. Parkin, L. Apostilco and K. C. Molloy, *J. Mater. Chem.*, 2001, **11**, 2408.
- 7 T. S. Lewkebandara, J. W. Proscia and C. H. Winter, *Chem. Mater.*, 1995, **7**, 1053.
- 8 F. A. Cotton, C. A. Murillo and M. A. Petrukhina, *J. Organomet. Chem.*, 2000, **593**, 1; F. A. Cotton, C. A. Murillo and M. A. Petrukhina, *J. Organomet. Chem.*, 1999, **573**, 78; F. A. Cotton, P. A. Kibala and W. A. Wojtczak, *Acta Crystallogr., Sect. C*, 1991, **47**, 89.
- 9 B. Patel, W. Levason, G. Reid, V. A. Tolhurst and M. Webster, *J. Chem. Soc., Dalton Trans.*, 2000, 3001.
- 10 F. A. Cotton, J. H. Matonic, C. A. Murillo and M. A. Petrukhina, *Inorg. Chim. Acta*, 1998, **267**, 173.
- 11 R. Hart, W. Levason, B. Patel and G. Reid, *Eur. J. Inorg. Chem.*, 2001, 2927.
- 12 *Auger and X-ray Photoelectron Spectroscopy (Practical Surface Analysis)*, eds. D. Briggs and M. P. Seah, Wiley, Chichester, 1990, vol. 1.
- 13 C. E. Myers, H. F. Franzen and J. W. Anderegg, *Inorg. Chem.*, 1985, **24**, 1822.
- 14 J. A. Rotole, K. Gaskell, A. Comte and P. M. A. Sherwood, *J. Vac. Sci. Technol. A.*, 2001, **19**, 1176.
- 15 I. P. Parkin, S. A. O'Neill, A. Mills, N. Elliott and R. J. H. Clark, *J. Mater. Chem.*, 2002, submitted for publication.
- 16 SHELXTL PC, version 5.03, Siemens Analytical X-Ray Instruments Inc., Madison, WI, 1994.